Simulations of the p97 complex suggest novel conformational states of hydrolysis intermediates

Supplemental Material

I. DETAILS OF MD SIMULATIONS AND ANALYSIS

Density maps generated from SAXS experiments in [1] were modified to remove solvent contributions by first histogramming the density values and then removing those which corresponded to the first (and highest) peak, as suggested in [2]. This, along with formatting, was performed with SITUS, while secondary structure restraints were generated with VMD. To prevent the sudden introduction of large forces into the system, MDFF simulations were divided into four phases (for an illustration see Figure S1. In the first phase, a secondary structure restraint of k_μ =200 kcal/mol/rad^2 was consistently applied to the backbone ϕ and ψ angles, while the grid scaling factor ψ was increased from 0.005 kcal/mol to 0.5 kcal/mol in increments of 0.005 kcal/mol every 50 ps, for a total of 5 ns of simulation. These parameters of k_μ and ψ were then maintained for 1 ns to allow for equilibration. Over the following 2 ns, ψ was maintained at 0.5 kcal/mol while k_μ was reduced by 10 kcal/mol/rad^2 every 100 ps until the secondary structure restraint was completely removed. Finally, a 2 ns equilibration with only ψ=0.5 kcal/mol was performed. This created a total of 10 ns MDFF simulation time. Classical MD simulations showed this protocol created stable structures for the transition state (which already had the best correlation to experiments), however the increased level of protein rearrangement required in the pre- and post-hydrolysis resulted in less stable structures, thus the length of each phase of the MDFF simulation was doubled for a total MDFF simulation time of 20 ns. For the "Restrained ATP" simulations, two additional restraints per monomer were introduced. The first was between the CD atom of E141 and the CZ atom of R709 with a minimum at 3.8 Å, and the second between the CG of D179 and NE of R709 with a minimum of 3.1 Å (to mimic salt bridges observed in one monomer of an initial unrestrained MDFF simulations), with force constants increased from .1 to 10 kcal/mol/Å^2 over the timepoints from 1 ns to 10 ns of the first MDFF phase.

Following the MDFF phase each structure was stripped of solvent molecules and re-solvated and ionized to create box sizes that were more amenable to the new protein conformations. Histidine assignments were determined by the Check Side Chains plugin to VMD (http://2p2idb.cnrs-mrs.fr/checksidechains/checksidechains.html), minimization and relaxation of heavy atom restraints was performed as described above, and finally 50 ns of simulation. All simulations were performed with the MD package NAMD [3], with local non-bonded interactions truncated at 10 Å with a smoothing function initiated at 8 Å and particle-mesh Ewald with a fifth-order B-spline and maximum grid spacing of 1 Å used for long range electrostatics [4]. The SHAKE algorithm was used to constrain all hydrogen-containing bonds [5], allowing for the use of a 2 fs timestep. The NPT ensemble was simulated with temperature control maintained through the use of Langevin dynamics with a damping coefficient of 2 ps^{-1} and pressure control with a Langevin piston with a target pressure of 1.01325 bar, a piston period of 100 fs, a damping time-scale of 50 ps, and a piston temperature of 300 K [6, 7].

The SITUS program colacor (which has been renamed to collage in the current SITUS version) was used to refine the position of atomic coordinates within, and compute the linear correlation to the SAXS density maps, as are present in Figure 4. The "inter-domain" angle, which was originally defined by Davies *et al.* [8], is the angle between the C_α atom of residue 107 (in the N domain), and the C3* atom of the nucleotides bound to the D1 and D2 domains, while the D2 α/β rotation angle was computed by first aligning the hexamer such that the central pore was along the z-axis, and measuring the angle between two vectors: one defined by the center of masses of the Nb and D1 domains of monomers on opposing sides of the hexamer and one by the center of masses of the D2 α/β domains of monomers on opposing sides of the hexamer. Figure 2 presents timecoureses for the averages over the monomers for each of these two angles. To compute the pore width in Figure 3 and S6 the hexamer was aligned along the z-axis and the program Hole was used [9]. Root mean square fluctuations (RMSF) and the Pearson correlation coefficients of the C_α atoms were computed over the final 20 ns of the MD simulations with the program Gromacs [10–12]. For calculations of correlations throughout the hexamer (S8), the final 40 ns was used. For RMSF calculations, each monomer was aligned to the coordinates of one monomer following MDFF simulations, and the average RMSF values from the six monomers are reported in Figure 5, while for cross-correlation analysis trajectories of each monomer, along with its clockwise neighbor, were concatenated, aligned based on the monomer's C_α atoms, and the covariance matrix for the entire dimer was computed. Root mean square deviations (RMSD) were computed using the VMD plugin RMSDTT

(http://physiology.med.cornell.edu/faculty/hweinstein/vmdplugins/rmsdtt) and molecular representations shown in Figure 1 were generated with VMD [13]. Hydrogen bonds were computed over the final 20 ns of the conventional MD simulations and defined by a distance cutoff of 3.5 Å between the donor and acceptor atoms, along with a 30° donor-hydrogen-acceptor angle cutoff.

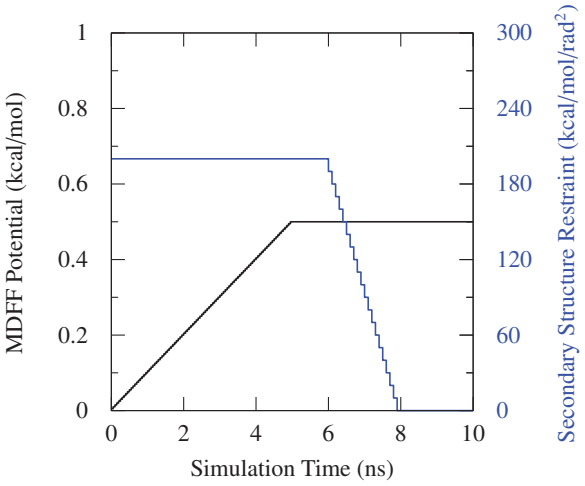

FIG. S1. Protocol for MDFF simulations

[1] J. M. Davies, H. Tsuruta, A. P. May, and W. I. Weis, Structure **13**, 183 (2005).
[2] L. G. Trabuco, E. Villa, K. Mitra, J. Frank, and K. Schulten, Structure **16**, 673 (2008).
[3] J. C. Phillips, R. Braun, W. Wang, J. Gumbart, E. Tajkhorshid, E. Villa, C. Chipot, R. D. Skeel, L. Kale, and K. Schulten, J. Comp. Chem. **26**, 1781 (2005).
[4] T. Darden, D. York, and L. Pedersen, J. Chem. Phys. **98**, 10089 (1993).
[5] V. Krautler, W. F. Van Gunsteren, and P. H. Hunenberger, J. Comp. Chem. **22**, 501 (2001).
[6] G. J. Martyna, D. J. Tobias, and M. L. Klein, J. Chem. Phys. **101**, 4177 (1994).
[7] S. E. Feller, Y. H. Zhang, R. W. Pastor, and B. R. Brooks, J. Chem. Phys. **103**, 4613 (1995).
[8] J. M. Davies, A. T. Brunger, and W. I. Weis, Structure **16**, 715 (2008).
[9] O. S. Smart, J. M. Goodfellow, and B. A. Wallace, Biophys. J. **65**, 2455 (Dec 1993).
[10] T. Ichiye and M. Karplus, Proteins **11**, 205 (1991).
[11] P. H. Hünenberger, A. E. Mark, and W. F. van Gunsteren, J. Mol. Biol. **252**, 492 (Sep 1995).
[12] E. Lindahl, B. Hess, and D. van der Spoel, J. Mol. Mod. **7**, 306 (2001).
[13] W. Humphrey, A. Dalke, and K. Schulten, J. Mol. Graphics **14**, 33 (1996).

II. ADDITIONAL DATA

	Monomer	N Domains			D1 Domains			D2 Domains		
		Whole	Na	Nb	Whole	α/β	α	Whole	α/β	α
ATP relative to Transition	13.72	7.00	7.79	2.61	4.89	3.85	4.21	8.93	5.62	9.02
Transition relative to ADP	9.85	6.16	6.88	2.58	3.39	2.86	3.28	6.40	4.17	7.22
ADP relative to ATP	9.02	5.53	6.54	2.62	4.57	3.95	4.15	7.59	5.01	7.93

TABLE S1. Heavy atom RMSD values between final structures for each hydrolysis state (in Å). The Na and both α subdomains undergo the largest conformational changes as hydrolysis proceeds, while Nb and the D1 α/β are relatively unchanged.

	ATP State				Transition State				ADP State			
	Hexamer	N	D1	D2	Hexamer	N	D1	D2	Hexamer	N	D1	D2
Crystal Relative to MDFF	0.40	0.30	0.28	0.36	0.16	0.37	0.18	0.31	0.20	0.39	0.21	0.32
Final Relative to MDFF	0.14	0.29	0.20	0.21	0.13	0.35	0.18	0.26	0.15	0.34	0.17	0.26
Final Relative to Crystal	0.35	0.30	0.24	0.34	0.14	0.42	0.13	0.25	0.16	0.34	0.17	0.24

TABLE S2. Heavy atom ρ_{sc} values. For each hydrolysis state, the ρ_{sc} values for the entire hexamer, and the average for the N, D1, and D2 domains are presented for the final MD structure relative to the crystal and final MDFF structures, as well as the crystal structure relative to the MDFF structure.

	D2 Nucleotide-R635	D2 Nucleotide-R638
ATP State	47.8% (3)	25.1 % (1)
Transition State	84% (5)	11.6% (1)
ADP State	30.4% (2)	15.2%(1)

TABLE S3. Average hydrogen bond occupancies of inter-protomer contacts between R635 and R638 and the nucleotide of the neighboring monomer. Arginine 635 appears to serve a larger role then 638 as the "arginine finer," however there does exist some contact between the nucleotide and R638.

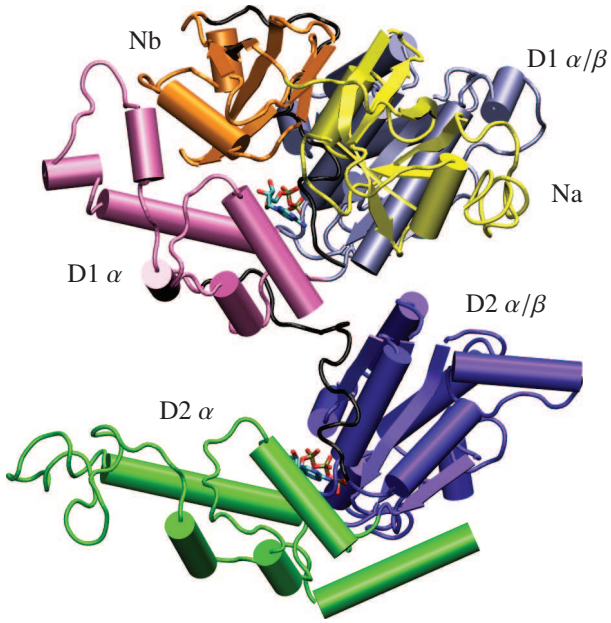

FIG. S2. Monomeric structure of p97 bound to ATP in both hydrolysis domains. The N domain consists of the Na (yellow) and Nb (orange), while each hydrolysis domain is subdivided into an α/β and α subdomain, colored blue and pink in D1 and purple and green in D2. Domains are linked by linker regions (shown in black).

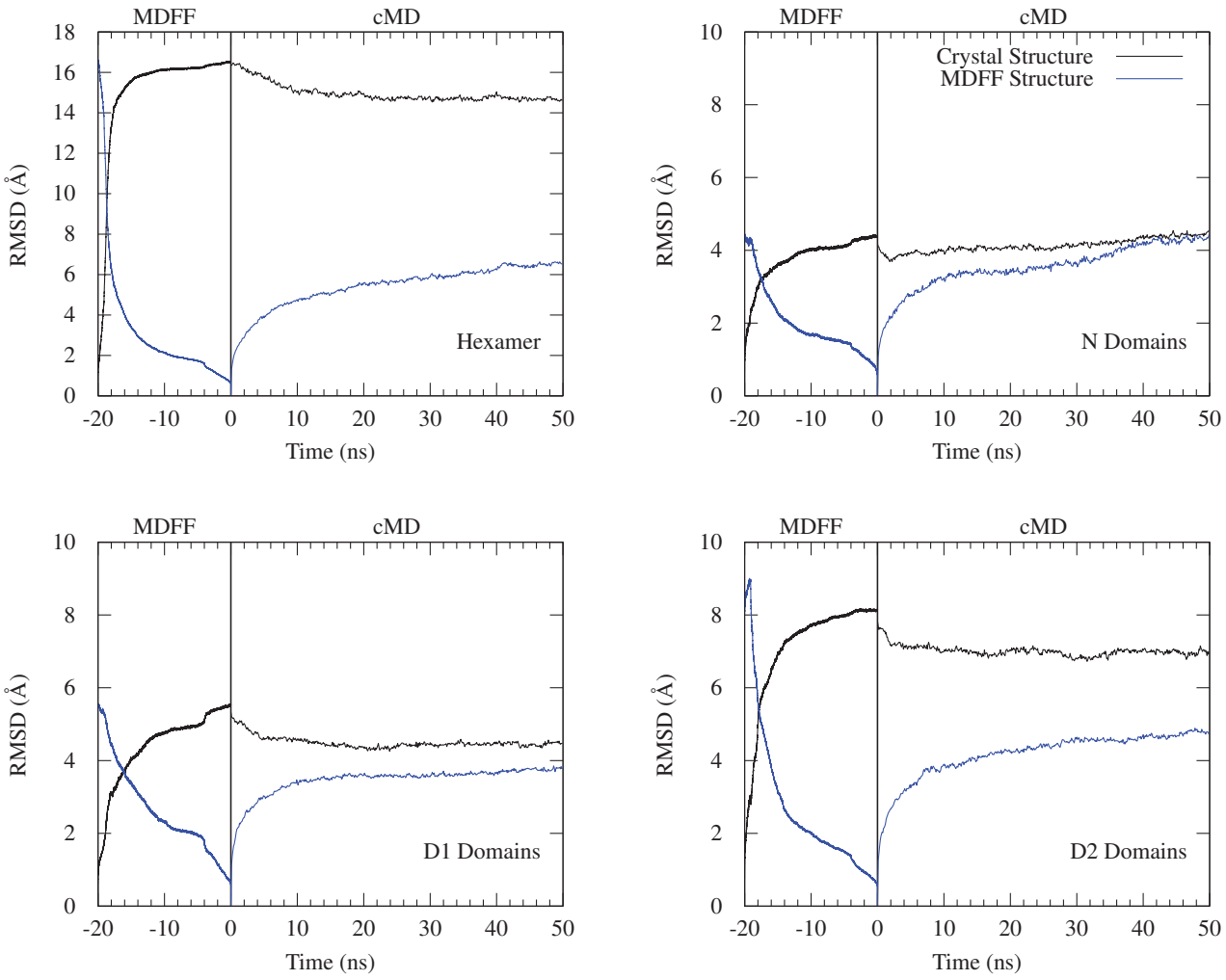

FIG. S3. RMSD For ATP State

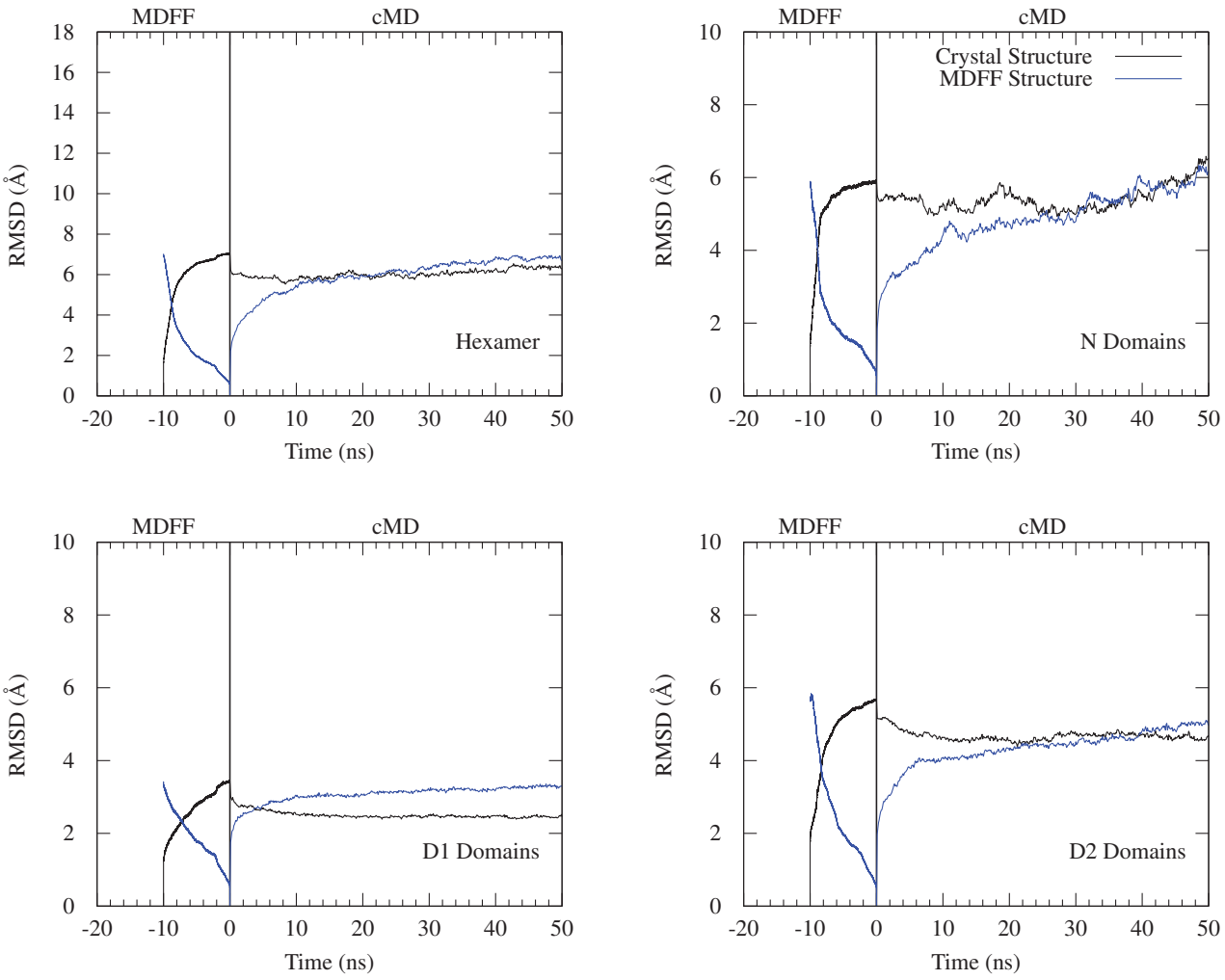

FIG. S4. RMSD For Transition State

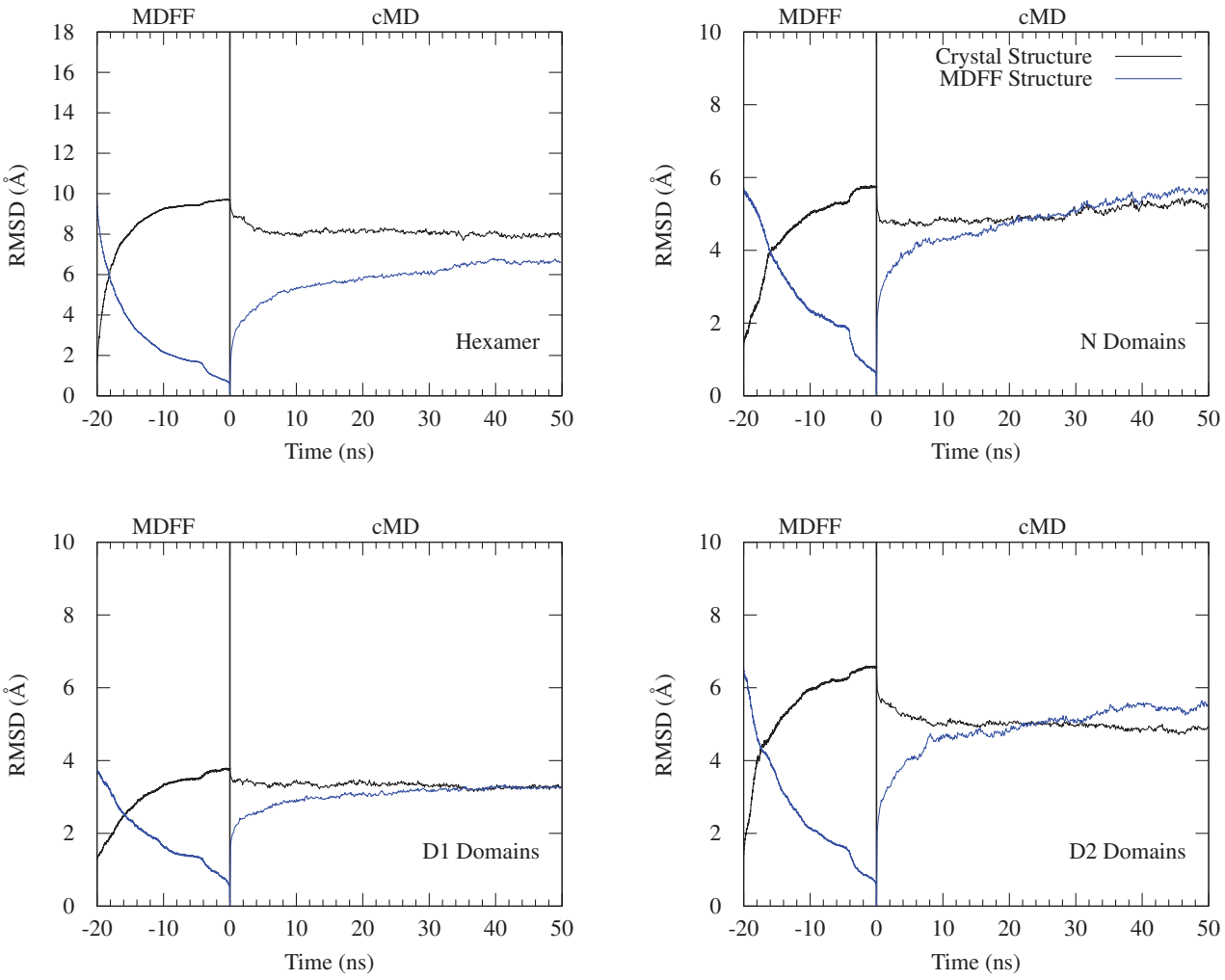

FIG. S5. RMSD For ADP State

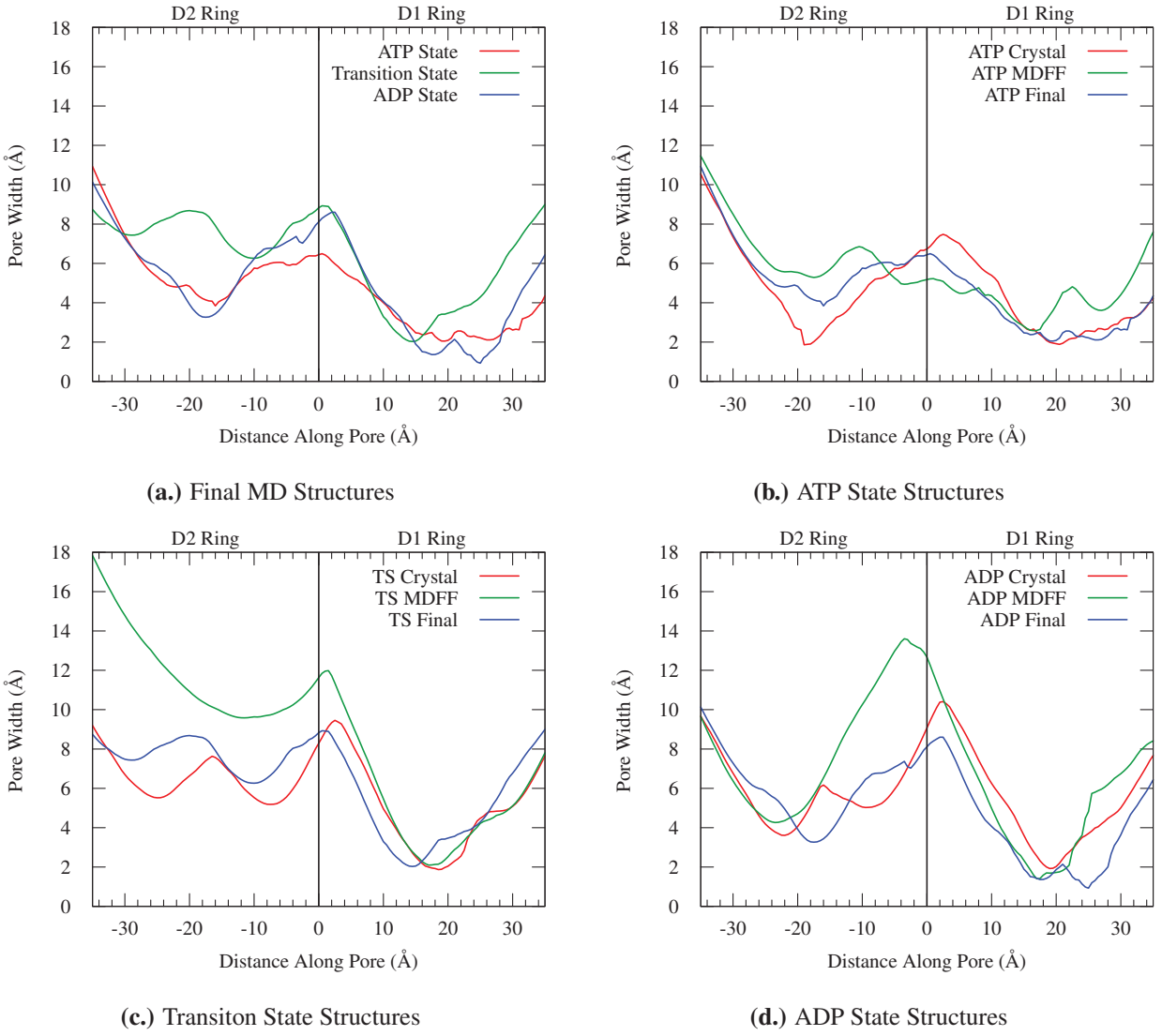

(a.) Final MD Structures

(b.) ATP State Structures

(c.) Transiton State Structures

(d.) ADP State Structures

FIG. S6. Radius of the central pore at points measured along its axis. **a.** The final structures from MD simulations have D2 pores which are more open than their D1 counterparts, especially in the case of the transition state. All three states have a maximum opening around the D1/D2 interface. For the individual states (**b.-d.**) the MDFF calculations produce structures with larger pore openings than in the crystal structures, however in the MD simulations he hexamers relax to structures with pores similar to those in the crystal structure.

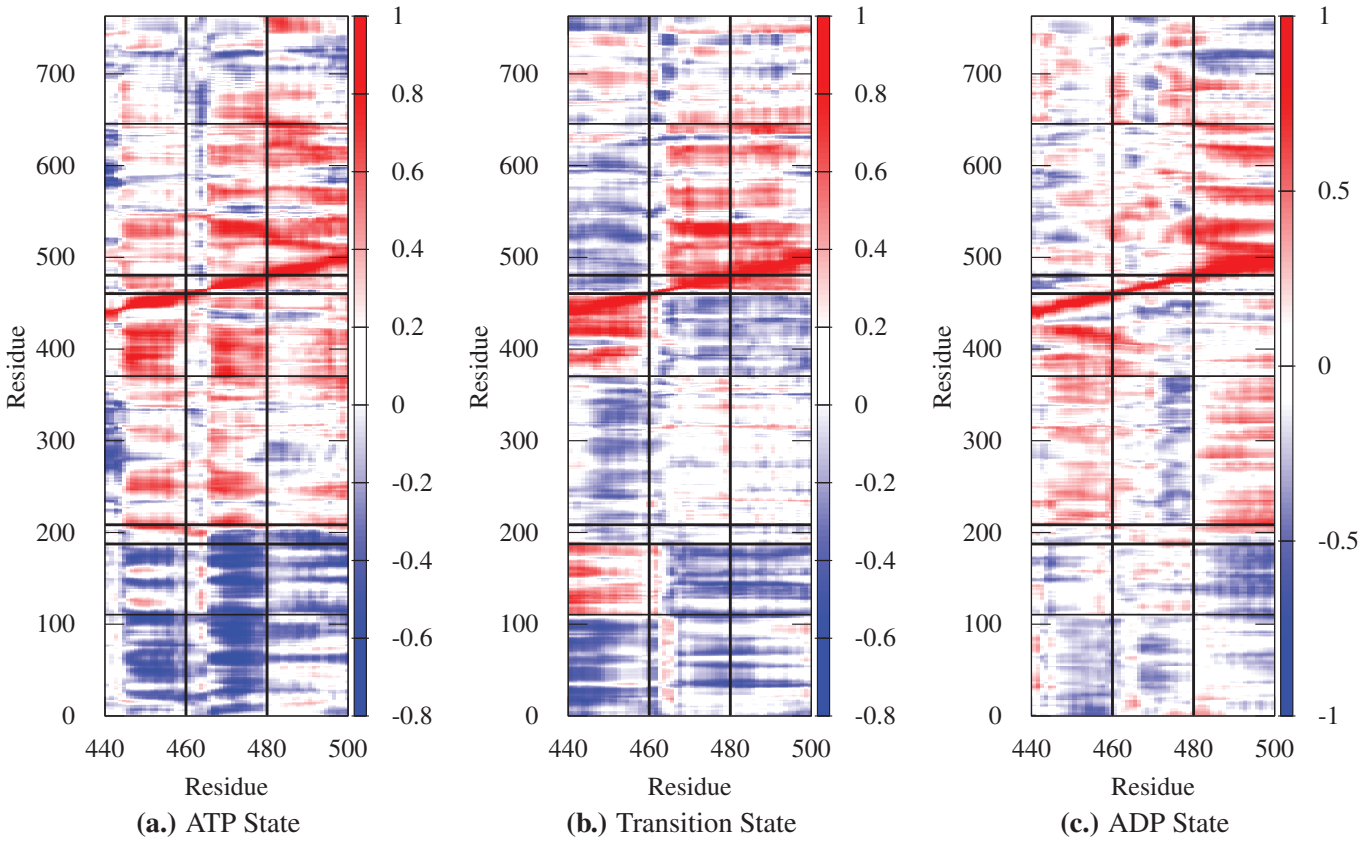

FIG. S7. Zoomed in cross correlation plots (from Figure 6) around the D1/D2 linker region.

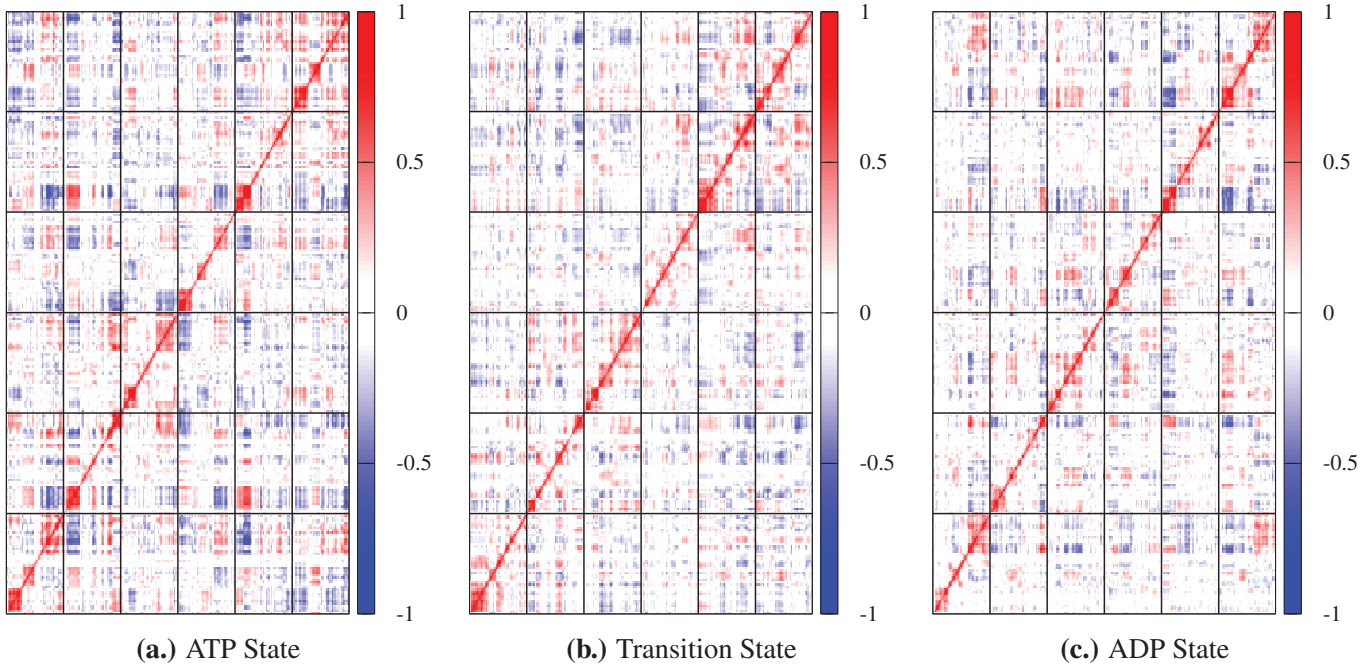

FIG. S8. Cross correlation plots for the entire hexamers. Note that to improve samplingi, the final 40 ns of simulation was utilized.

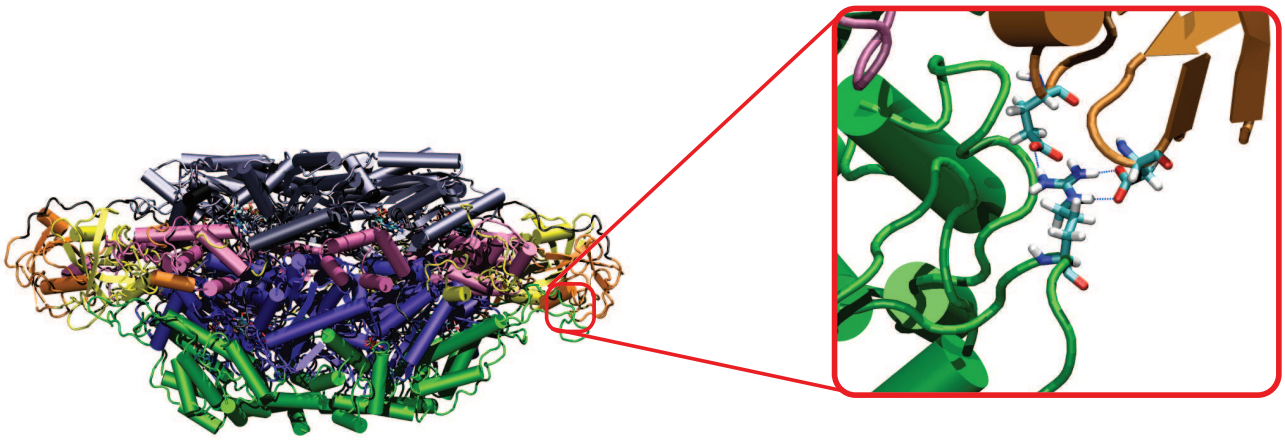

FIG. S9. The location of salt bridges between R709 and E141/D179 in the pre-hydrolysis state